Intermolecular polarizabilities in H2-rare-gas mixtures (H2–He, Ne, Ar, Kr, Xe): Insight from collisional isotropic spectral properties

Waldemar Glaz, Tadeusz Bancewicz, Jean-Luc Godet, Magnus Gustafsson, George Maroulis, Anastasios Haskopoulos

Intermolecular polarizabilities in H_2-rare-gas mixtures (H_2–He, Ne, Ar, Kr, Xe): Insight from collisional isotropic spectral properties

Waldemar Głaz,[1,a)] Tadeusz Bancewicz,[1] Jean-Luc Godet,[2] Magnus Gustafsson,[3] George Maroulis,[4] and Anastasios Haskopoulos[4]
[1]*Nonlinear Optics Division, Faculty of Physics, Adam Mickiewicz University, Umultowska 85, 61-614 Poznań, Poland*
[2]*Laboratoire de photonique d'Angers, Université d'Angers, 2 boulevard Lavoisier, 49045 Angers, France*
[3]*Department of Chemistry and Molecular Biology, University of Gothenburg, SE 412 96 Gothenburg, Sweden*
[4]*Department of Chemistry, University of Patras, GR-26500 Patras, Greece*

(Received 12 May 2014; accepted 31 July 2014; published online 20 August 2014)

The report presents results of theoretical and numerical analysis of the electrical properties related to the isotropic part of the polarizability induced by interactions within compounds built up of a hydrogen H_2 molecule and a set of noble gas atoms, Rg, ranging from the least massive helium up to the heaviest xenon perturber. The Cartesian components of the collisional polarizabilities of the H_2–Rg systems are found by means of the quantum chemistry methods and their dependence on the intermolecular distance is determined. On the basis of these data, the spherical, symmetry adapted components of the trace polarizability are derived in order to provide data sets that are convenient for evaluating collisional spectral profiles of the isotropic polarized part of light scattered by the H_2–Rg mixtures. Three independent methods of numerical computing of the spectral intensities are applied at room temperature (295 K). The properties of the roto-translational profiles obtained are discussed in order to determine the role played by contributions corresponding to each of the symmetry adapted parts of the trace polarizability. By spreading the analysis over the collection of the H_2–Rg systems, evolution of the spectral properties with the growing masses of the supermolecular compounds can be observed. © *2014 AIP Publishing LLC*. [http://dx.doi.org/10.1063/1.4892864]

I. INTRODUCTION

The light scattering processes determined by intermolecular correlations and interactions (collision-induced light scattering, CIS) have attracted considerable attention for a number of decades and still belong to the core area of interest of many experimental and theoretical groups.[1] The so-called depolarized collisionally-induced light scattering (DCIS), attributed to the anisotropic part of the polarizability tensor of an active supermolecule, was the first effect of this kind observed in the media composed of noble gas atoms;[2] and the extraction of the polarized, isotropic component of the induced scattering (ICIS) intensity, related to the trace of the polarizability, was to follow after several years.[3] Even though both phenomena have become the subject of thorough research, the ICIS process is significantly less explored in comparison with DCIS. This situation was mainly due to the experimental limitations and very weak intensities of the isotropic contribution to the scattered radiation as the polarized spectrum turned out to be much weaker and broader than its anisotropic counterpart. In addition, it could not be obtained directly from the measured intensities, but it had to be calculated by subtraction of two values of similar magnitude, which usually resulted in substantial experimental uncertainties.[4–6] Even more significant hurdles were encountered, when the spectra were measured in molecular gases, such as hydrogen. In that case, the additional difficulty stemmed from the presence of allowed rotational Raman transitions, which obscured the diffuse collisional contributions. Nonetheless, such spectra were analyzed in a number of systems including noble gas atoms and diatoms,[1,7–9] hydrogen and deuterium molecules,[6,10–12] and more complex systems, such as H_2O[13,14] and H_2S.[15,16] The Rayleigh isotropic spectra were also studied in N_2 gas,[17] CF_4, CH_4, or SF_6 species.[18–21]

Meanwhile, the measuring methods and tools of molecular spectroscopy have achieved unprecedented sophistication and their level of accuracy provided opportunities for detection of very weak signals (e.g., Refs. 9 and 22). Significant progress has also been made in the *ab initio* numerical methods of quantum chemistry[23–30] with regard to ability of determining the collisional electrical properties; similar development has improved to great extent theoretical/numerical procedures of evaluating CIS spectral profiles.[31–33]

The above realization has called forth anew the question of mechanisms responsible for inducing the collisional properties determining the nature of radiative phenomena following from the isotropic polarizability. The feasibility of more precise measurements of polarized intensities has evoked the need of appropriate theoretical and numerical interpretation tools. In this study, an apparatus of that kind has been assembled in order to calculate the collisional polarizabilities and evaluate the connected roto-translational ICIS spectra of the light scattered by mixtures composed of diatomic hydrogen molecules and a complete set of noble gas atoms (except for Rn).

a)Author to whom correspondence should be addressed. Electronic mail: glaz@kielich.amu.edu.pl

Such a choice of the scattering systems to consider seems rather obvious, physically and historically. The noble gas media were among the first atomic species in which the ICIS effect was detected; whereas hydrogen, is among the most popular molecular scatterers and absorbers for its relative computational simplicity and importance for astrophysical research.[34,35] Additionally, the quantum features of H_2 as a quantum rotator with a large rotational constant make this molecule a convenient object of spectral measurements of relatively weak effects, for instance ICIS, which otherwise could be masked by much pronounced signals.

Moreover, since the earliest empirical measurements of ICIS, it has been known that the properties of the noble gas spectra may noticeably differ from those of hydrogen lines. This is usually accounted for by a hierarchy of importance among the types of interactions responsible for inducing collisional properties, especially, as far as the range of forces is considered.[6,12] In view of this conclusion, it appears as a rather natural idea to have a better theoretical insight into relevant properties of the systems that combine the qualities of H_2 and Rg. For example, this kind of research gives a good opportunity to observe a gradual evolution of the electrical properties and related spectra with the growing mass of noble gas moieties.

It is also worth noting that similar research into the electrical features of H_2–Rg supermolecules was earlier undertaken for collision-induced dipole moments of H_2–He and H_2–Ar mixtures in works considering the collisional induced absorption effects, mainly in an astrophysical context.[36–40] To the best of our knowledge none of the remaining pairs, with Rg = Ne, Kr, and Xe, have received much attention in reports on collisional absorption yet published. Besides, a series of articles devoted to the so-called hyper-Rayleigh collisional scattering have appeared in which a comparative study on the evolution of collisional properties (hyperpolarizabilities in this case) within the whole set of the H_2–Rg compounds is discussed.[41–47]

The ideas formulated in the previous paragraphs find their practical realization in this work. Namely, Sec. II sheds light on the importance of theoretical determination of the trace of the collisional polarizabilities in interpreting possible experimental results of the isotropic scattering signals. General description of the methodology of expressing these properties in terms of both Cartesian and spherical tensor approach is presented in Sec. III. In Sec. IV, the *ab initio* methods of quantum chemistry are applied to determine a functional dependence of Cartesian components of the trace polarizability of H_2–Rg systems on the intermolecular distance. The Cartesian values are subsequently transformed into the so-called symmetry adapted (SA) spherical components[33] suitable for calculating spectral shapes of the isotropic collisional scattering. Appropriate expressions defining the intensities of the scattered light are presented in Sec. V, where three different schemes of evaluating the desired ICIS profiles are proposed: the quantum mechanical[48] (QM), semi-classical[48] (SC), and close coupling[11,49] (CC) approach. The calculations are performed under certain assumptions with regard to the properties of the scattering systems. Foremost, only the binary, two molecule collisions are taken into account. Second, the isotropic potential approximation (IPA) is applied at the first stage of analysis. Additionally, in the CC computing procedure, the anisotropy of the potentials can be also "switched on," so that the influence of the angular dependence of the interactions could be estimated. Finally, the calculated polarizabilities and related spectral profiles are presented and their interpretation is given in the concluding paragraphs of the work in Sec. VI.

II. COLLISION-INDUCED ISOTROPIC SPECTRUM: GENERAL CONSIDERATIONS

Let us consider the light scattering experimental setup. The directions of the incident and scattering beams define the scattering plane. The scattered light is observed at the right angle with respect to the incident beam. If one assumes two independent light scattering intensity measurements, one with laser polarization perpendicular to the scattering plane ($\mathcal{J}_V(\omega)$) and the second one with the laser polarization parallel to the scattering plane ($\mathcal{J}_H(\omega)$). No analyzer is used. The anisotropic and isotropic intensities, $\mathcal{D}(\omega)$ and $\mathcal{J}_{iso}(\omega)$, may be obtained from the measured intensities $\mathcal{J}_V(\omega)$ and $\mathcal{J}_H(\omega)$ and from the following equations:[1,50]

$$\begin{aligned} \mathcal{J}_H(\omega) &= a\,\mathcal{J}_{iso}(\omega) + d\,\mathcal{D}(\omega), \\ \mathcal{J}_V(\omega) &= c\,\mathcal{J}_{iso}(\omega) + b\,\mathcal{D}(\omega), \end{aligned} \tag{1}$$

where a, b, c, and d are coefficients dependent on the angle used to collect the scattering beam. For instance, if its value is set to 90°, $a = 0$, $b = 7/6$, and $c = d = 1$. However, in a realistic situation, a detector has finite dimensions, which modifies the actual values of the coefficients.[51] The isotropic spectrum cannot be measured directly, yet on the grounds of the equation set, Eq. (1), it can be determined as a weighted difference of the $\mathcal{J}_V(\omega)$ and $\mathcal{J}_H(\omega)$ spectral intensities.[52] Theoretically, the CI isotropic spectrum is computed if the isotropic part of the CI polarizability tensor is known.

III. COLLISION-INDUCED POLARIZABILITY: THEORETICAL OUTLINE

A. Cartesian approach

The present calculation of the interaction-induced electric properties of the H_2–Rg (Rg = He, Ne, Ar, Kr, and Xe) pairs leans heavily on previous experience on He–He, Ne–Ne, Ar–Ar, Kr–Kr, H_2–H_2, Ne–HF,[23] CO_2–Rg,[24] Ne–Ar,[25] Xe–Xe,[53] Kr–Xe,[26] and Rg–He.[54] Only a few essential points of the computational approach are given here. The energy E_p of an uncharged molecule in a weak, homogeneous static electric field can be expanded as[55]

$$\begin{aligned} E_p = E_0 - \mu_\alpha F_\alpha - (1/2)\alpha_{\alpha\beta} F_\alpha F_\beta - (1/6)\beta_{\alpha\beta\gamma} F_\alpha F_\beta F_\gamma \\ - (1/24)\gamma_{\alpha\beta\gamma\delta} F_\alpha F_\beta F_\gamma F_\delta + \ldots, \end{aligned} \tag{2}$$

where $F_{\alpha\ldots}$ is the field, while E_0 is the energy of the free molecule. Here, the tensorial notation for the electric property is used: μ_α is the dipole moment, $\alpha_{\alpha\beta}$ is the dipole polarizability, $\beta_{\alpha\beta\gamma}$ is the first dipole, and $\gamma_{\alpha\beta\gamma\delta}$ is the second dipole hyperpolarizability. Basis set superposition error effects (BSSE) are removed by the counterpoise method of

Boys and Bernardi.[56] The subscripts denote Cartesian components and a repeated subscript implies summation over x, y, and z. The number of independent components needed to specify the above tensors is strictly regulated by symmetry.[57] In the calculations, three distinct configurations are chosen defined by the angle θ determining the orientation of the H_2 internuclear axis with regard to the vector connecting the mass centers of H_2 and Rg, namely, $\theta = 0°$, 45°, or 90°. The computational complexity varies considerably in each case, depending on the respective symmetry. Thus, the number of independent collisional components is:

- for $C_{\infty v}$ symmetry ($\theta = 0°$, linear or L-configuration), one for the dipole moment ($\Delta\mu_z$), two for the polarizability ($\Delta\alpha_{xx}$, $\Delta\alpha_{zz}$), and two for the first hyperpolarizability ($\Delta\beta_{xxz}$, $\Delta\beta_{zzz}$),
- C_s ($\theta = 45°$), two ($\Delta\mu_x$, $\Delta\mu_z$), four ($\Delta\alpha_{xx}$, $\Delta\alpha_{yy}$, $\Delta\alpha_{xz}$, $\Delta\alpha_{zz}$), and six ($\Delta\beta_{xxx}$, $\Delta\beta_{xyy}$, $\Delta\beta_{xxz}$, $\Delta\beta_{yyz}$, $\Delta\beta_{xzz}$, $\Delta\beta_{zzz}$)
- C_{2v} ($\theta = 90°$ or T-configuration), one ($\Delta\mu_x$), three ($\Delta\alpha_{xx}$, $\Delta\alpha_{yy}$, $\Delta\alpha_{zz}$), and three ($\Delta\beta_{xxx}$, $\Delta\beta_{xyy}$, $\Delta\beta_{xzz}$).

The components of the collisional polarizabilities listed above are computed by means of the QC methods described in Secs. IV and are subsequently applied as input data for the symmetry adapted calculations based on procedures discussed in Sec. III B below.

B. Spherical tensor representation

The values of the spherical components of the collision induced pair polarizability tensor, $\Delta\alpha$, for a system composed of a linear molecule and an atom (H_2–Rg in this work) are determined by the molecular orientation Ω_{H_2}($\equiv \theta$) with regard to the relative intermolecular separation vector $\boldsymbol{R}$. The $\Delta\alpha_\mu^{(K)}(\hat{\boldsymbol{R}}, \Omega_{H_2})$ dependence can be expressed as a series expansion in term of the spherical harmonics[58–60]

$$\Delta\alpha_\mu^{(K)}(\boldsymbol{R}, \Omega_{H_2}) = \frac{4\pi}{(2K+1)^{1/2}} \sum_{\lambda,L} \Delta\alpha_{\lambda L}^{(K)}(R) \times \{\mathbf{Y}_\lambda(\Omega_{H_2}) \otimes \mathbf{Y}_L(\hat{\boldsymbol{R}})\}_\mu^K. \quad (3)$$

If the vector, $\hat{\boldsymbol{R}}$, is assumed to be parallel to the reference frame z-axis, the spherical function $Y_{LM} = \sqrt{(2L+1)/4\pi}\,\delta_{M0}$. For the isotropic scattering, i.e., when $K = 0$, λ equals L and, consequently, Eq. (3) transforms to

$$\Delta\alpha_0^{(0)}(R) = \left(\frac{4\pi}{2K+1}\right)^{1/2} \sum_\lambda (2L+1)^{1/2}\, \Delta\alpha_{\lambda\lambda}^{(0)}(R) \times Y_{\lambda 0}(\Omega_{H_2})\, C_{\lambda 0 \lambda 0}^{00}, \quad (4)$$

where $C_{a\alpha\, b\beta}^{c\gamma}$ stands for the Clebsch-Gordan coefficient.[61] The coefficients $\Delta\alpha_{\lambda\lambda}^0(R)$ in Eq. (4) are the so-called symmetry adapted components of the collisional polarizability $\Delta\alpha$, which can be determined by considering three molecular arrangements: H_2 molecule is parallel to the axis z, H_2 molecule is perpendicular to the z axis, and molecule H_2 makes an angle of 45° with the z axis. As a result, a set of three independent equations, stemmed from Eq. (4), can be derived, from which the SA polarizability components: $\Delta\alpha_{00}^{(0)}(R)$, $\Delta\alpha_{22}^{(0)}(R)$, and $\Delta\alpha_{44}^{(0)}(R)$ are obtained. In the further course of the study, this allow us to compute the CI isotropic light scattering spectra for the H_2–Rg pairs.

IV. COLLISION-INDUCED POLARIZABILITIES: COMPUTING METHOD

The interaction quantity $P_{int}(H_2\text{–Rg})$ (the polarizability in this study) at a given position of the Rg atom, defined by $\boldsymbol{R} = (R, \theta)$, is computed as

$$P_{int}(H_2 - Rg) \equiv P_{int}(H_2 - Rg)(R) = P(H_2 - Rg)(R) - P(H_2 - X)(R) - P(X - Rg)(R). \quad (5)$$

The symbol $P(H_2 - Rg)(R)$ denotes the property P for $H_2 - Rg$. $P(H_2 - X)(R)$ is the value of P for subsystem H_2 in the presence of the ghost orbitals of the subsystem Rg, which appear in the Boys–Bernardi method and are adapted in this paper for the removal of the BSSE.[56]

The computational methods used in this paper are self-consistent field (SCF) and the conventional post-Hartree-Fock approaches second-order Møller-Plesset Perturbation Theory (MP2) and coupled-cluster theory with singles and doubles (CCSD). Detailed presentations of these methods are given in standard high-level textbooks.[57] Their performance in interaction electric properties has been carefully tested in previous work. See, for instance, work on CO_2–Rg,[24] Ne–Ar,[25] and He–Ne[62] for a comparison of CCSD to CCSD(T), which includes an estimate of connected triple excitations obtained via a perturbational treatment.

The choice of suitable basis sets for calculations of interaction-induced electric (hyper) polarizabilities deserves special attention.[63–66] In this work, atom-specific or molecule-specific purpose-oriented basis sets are exclusively used. In previous work, it has been shown that such basis sets are easily obtained for small systems such as atoms,[67] diatomics,[65,68] triatomics,[67,69] and small symmetrical polyatomics.[70,71]

Here, only a succinct presentation of the essential characteristics of the calculations performed for the pairs H_2–Rg (Rg = He, Ne, Ar, Kr, and Xe) is given. All calculations have been performed with the Gaussian[30,72] sets of programs.

- **H_2–He**. A full presentation of the computational effort on this system has been given in Ref. 73. The interaction-induced properties are calculated at the CCSD(Full) level of theory with a H_2/He = [6*s*4*p*3*d*1*f*/6*s*4*p*3*d*1f] basis set. Both the dihydrogen and helium parts are augmented versions of the [6*s*4*p*1*d*] basis used on H_2–H_2 and the [6*s*4*p*3*d*] one used on He–He.[23]
- **H_2–Ne**. The calculations were performed at the CCSD(Full)/ [6*s*4*p*3*d*/7*s*5*p*4*d*1*f*] level of theory. The H_2 = [6*s*4*p*3*d*] basis set is an augmented version of the basis set used on calculations on H_2–H_2 and Ne = [7*s*5*p*4*d*1*f*] the basis used for the calculation of the interaction-induced properties of the Ne–Ne pair.[23]
- **H_2–Ar**. Some computational details have been given in previous work.[74] All calculations were performed

at the MP2(FC)/[6*s*4*p*2*d*/8*s*6*p*5*d*4*f*] level of theory. The ten innermost MO were kept frozen. The H_2 = [6*s*4*p*2*d*] basis is an augmented version of the [6*s*4*p*1*d*] one used on calculations on H_2-H_2 and [8*s*6*p*5*d*4*f*] is the basis used for the calculation of the interaction-induced properties of the Ar–Ar pair.[23]

- **H_2–Kr**. Computational aspects of the calculations on H_2–Kr will appear in a separate paper. The calculations were performed at the CCSD(FC)/[6*s*4*p*3*d*/8*s*7*p*6*d*1*f*] level of theory with the nine innermost MO frozen. The H_2 part is the same as the one used on H_2–Ne, see above. The Kr = [8*s*7*p*6*d*1*f*] basis is the one used for the calculation of the interaction-induced properties of the Kr–Kr pair.[23]
- **H_2–Xe**. A detailed presentation of the calculations on H_2–Xe will be given elsewhere. All calculations were performed at the CCSD(FC)/[6*s*4*p*3*d*/9*s*8*p*7*d*1*f*] level of theory with the 18 innermost MO frozen. The H_2 = [6*s*4*p*3*d*] basis is the same as for H_2–Kr. The basis set on Xe = [9*s*8*p*7*d*1*f*] is an atom-specific, purpose-oriented basis set.[26]

In the following step, the Cartesian polarizabilities obtained by the procedures described above are converted to the symmetry adapted spherical components. Eventually, the later quantities are fitted to a functional form suitable in the spectral profiles computing schemes applied in the section hereafter. The details of the fitting routines are given in Refs. 42–44.

V. SPECTRAL CONSIDERATIONS AND CALCULATIONS

In general, the potential of interaction between the moieties of the H_2–Rg systems is the anisotropic, angular-dependent, property that typically is expressed in the form of Legendre expansion[75]

$$V(\mathbf{r}, \boldsymbol{R}) = \sum_{\gamma} V_{\gamma}(R, r)\ P_{\gamma}(\widehat{\mathbf{r}} \cdot \widehat{\boldsymbol{R}}), \tag{6}$$

where $\boldsymbol{r}$ is the bond axis vector of H_2. The subscripts γ are even integers due to the inversion symmetry of the H_2-molecule. However, quite often, it can be safely assumed that for the supermolecular compounds consisting of hydrogen molecules the influence of the anisotropic part of V is rather weak.[36,76] On the other hand, some of the spectral features of collisional absorption processes in the mixtures of H_2 and Rg components were seen as quite significantly accounted for by the anisotropy of the systems.[39,40,77] Therefore, although the isotropic potential approximation approach is also domineering in the analysis to follow, more careful attention will be also given to a possible role of the anisotropic interactions in shaping the properties of the supermolecules and the performance of the effects studied. In the calculations presented below, a number of potential surfaces are applied for the systems considered: the Schaefer and Kohler model[75] for H_2–He, Lique's evaluation[78] for H_2–Ne, the functions provided by Williams *et. al.* for H_2–Ar,[79] and those published by Le Roy and Hutson in the H_2–Kr/Xe cases.[80]

A. Isotropic potential approximation

When the spherical symmetry approximation of the interactions is taken into account, the H_2 molecules can be regarded as free linear rotators, of which angular motion may be treated separately from the translational degrees of freedom characterizing the intermolecular motion of H_2 and Rg. On this assumption, the relevant polarizability autocorrelation function $F(t)$ of the radiation scattered by a sample of volume V can be split into a product of the rotational, $R^{rot}(t)$, and the translational, $S^{tr}(t)$, components[58,81–83]

$$F(t) = \frac{1}{V}\, R^{rot}(t)\, S^{tr}(t). \tag{7}$$

Hence, the spectral distribution of the scattered light intensity expressed by the differential light scattering cross section per pair of colliding entities can be written as a series of convolutions of the Fourier transforms of $R^{rot}(t)$ and $S^{tr}(t)$ functions[1,10,83,84] related to a specific SA polarizability component $\Delta\alpha^{(0)}_{\lambda\lambda}$,

$$\begin{aligned} \mathcal{J}_{iso}(\omega) &= V \left(\frac{\partial^2 \sigma}{\partial \Omega \partial \omega} \right)_{iso} \\ &= k_s^4 \sum_{\lambda} \int R^{(0)}_{\lambda}(\omega')\ g^{(0)}_{\lambda\lambda}(\omega - \omega')\, d\omega', \end{aligned} \tag{8}$$

In the equations above, the frequencies are shifted with respect to a laser line of wavelength λ_0 (in present calculations, the green line of wavelength $\lambda_0 = 514.5$ nm is used), $\omega = \omega_0 - \omega_s$, and the spectral distributions are normalized with the incident energy flux of the laser beam, while k_s denominates the wave vector magnitude of the scattered signal at the frequency ω_s. It is noteworthy here that, depending on the experimental context, the coefficient k_s^4 is often replaced by $k_0 k_s^3$. Namely, when photon counting measurements are analyzed, the definition in Eq. (8) should be multiplied by the scale factor $\kappa = k_0/k_s$. The two conventions, however, are fully convertible by applying this multiplier, which usually does not exceed unity by more than 2% .[83] In this work, the photon counting approach is found more appropriate in the close coupling considerations of Sec. V B.

The rotational contribution to the spectrum can be derived on the grounds of the standard quantum mechanics procedures yielding[42,85]

$$\begin{aligned} R^{(0)}_{\lambda}(\omega) = \frac{1}{3} \sum_{j_i, j_f} (2j_i + 1)(2j_f + 1) g_{j_i} \frac{\exp\left(-E^{rot}_{j_i}/k_B T\right)}{Z} \\ \times \begin{pmatrix} j_i & \lambda & j_f \\ 0 & 0 & 0 \end{pmatrix}^2 \delta(\omega - \omega_{j_i j_f}) \end{aligned} \tag{9}$$

with the rotational energy of H_2 molecules $E^{rot}_j = B\, j(j+1)$ and the frequency shift defined as $\omega_{j_i j_f} = -(E_{j_f} - E_{j_i})/\hbar$, where i and f indices are used to mark the initial and final state, respectively. The coefficient $\begin{pmatrix} j & \lambda & j' \\ 0 & 0 & 0 \end{pmatrix}$ denotes the

3–j Wigner symbol,[61,86] Z is the rotational partition function, g_j is the nuclear-statistical weight ($g_j = 1$ for even j in para-H_2 and g_j=3 for odd j in ortho-H_2), while B stands for the rotational constant of the hydrogen molecule. Note that $(2j+1)\begin{pmatrix} j & \lambda & j' \\ 0 & 0 & 0 \end{pmatrix}^2$ is exactly the Placzek-Teller factor[48] for a rotating linear molecule. The expression given in Eq. (9) determines a spectral distribution of a discrete set of intensities that are to be *enveloped* with an appropriate translational ($\boldsymbol{R}$-motion related) profiles, ${}^{(QM,cl)}g^{(0)}_{\lambda\lambda}(\omega)$, in order to produce—via the formula in Eq. (8)— the overall roto-translational line shape. The main procedure applied in this study to achieve this goal is based on numerical integration of the Schrödinger equation determining the relative motion of the supermolecule components interacting with an isotropic pair potential. These results are supplemented with the intensities obtained by two other independent methods: the semi-classical routines and the close-coupling approach used partially as a benchmarking tool testing the reliability of the spectral profiles obtained. The details of these computing schemes are given in a number of previously published works. Therefore, in Secs. V A 1–V B, a succinct description is only provided addressing the steps adapted to the specific requirements of the radiating effects analyzed.

1. Quantum mechanical computing of translational spectral profiles: IPA case

In this method, the spectral density function associated with the relative translational motion is defined as[1,48,58,87]

$$
\begin{aligned}
{}^{(QM)}g^{(K)}_{\lambda L}(\omega) = V \sum_{i,f} (2l_i+1)\, b(L)^{l_f}_{l_i}\, P_i \int_0^\infty \Big| \Psi^*(R;E_f,l_f) \\
\times \Delta\alpha^{(K)}_{\lambda L}(R) \Psi(R;E_i,l_i)\, dR \Big|^2 \\
\times \delta(\omega - \omega_{if}),
\end{aligned}
\tag{10}
$$

where the partial wave-functions Ψ are related to the solutions of the radial Schrödinger equation normalized according to boundary values 0 as $R \to 0$ and $\sin(kR - l\pi/2 + \delta_l)$ as $R \to \infty$.[48] Again, in this expression the Placzek-Teller factor appears

$$
b(L)^{l'}_{l} \equiv (2l'+1) \begin{pmatrix} l' & L & l \\ 0 & 0 & 0 \end{pmatrix}^2, \tag{11}
$$

this time corresponding to the angular degrees of freedom characterizing the orientation of the vector $\boldsymbol{R}$, while P_i denotes the probability of finding the sample in the initial state i. After having performed the steps usually applied in such calculations (see, e.g., Refs. 10–12, 88, and 89) the following form of the spectral function can be found in a more workable form:

$$
\begin{aligned}
{}^{(QM)}g^{(K)}_{\lambda L}(\omega) \\
= \lambda_0^3 \left(\frac{2\mu}{\hbar\pi^2}\right) \sum_{l_i,l_f} (2l_i+1)\, b(L)^{l_f}_{l_i} \\
\times \int_0^\infty \frac{dE_i}{(E_i E_f)^{1/2}} \Big[\exp(-E_i/k_B T) \\
\times \Big| \int_0^\infty \Psi^*(R;E_f,l_f)\, \Delta\alpha^{(K)}_{\lambda L}(R)\, \Psi(R;E_i,l_i)\, dR \Big|^2 \Big],
\end{aligned}
\tag{12}
$$

where the summation over the states, i and f, is converted into an integral over energies. Usually, a further refinement of the expression is achieved by having recourse to the so-called energy normalization[58,83,90] of the wave functions (now denoted $\hat{\Psi}$), which results in the following equation:

$$
\begin{aligned}
{}^{(QM)}g^{(0)}_{\lambda\lambda}(\nu) \\
= 2\pi\hbar c \lambda_0^3 \sum_{l_i,l_f} (2l+1)\, b(\lambda)^{l_f}_{l_i} \int_0^\infty dE_i \Big[\exp(-E_i/k_B T) \\
\times \Big| \int_0^\infty \hat{\Psi}^*(R;E_f,l_f)\, \Delta\alpha^{(0)}_{\lambda\lambda}(R)\, \hat{\Psi}(R;E_i,l_i)\, dR \Big|^2 \Big],
\end{aligned}
\tag{13}
$$

additionally specified for the case of the isotropic scattering, i.e., for $K = 0$. Herein above, the indexes i and f determine the quantum states of the system determined by the energies E and the quantum angular momentum number l of the relative motion of H_2 and Rg; λ_0—the thermal de Broglie wavelength—is defined by

$$
\lambda_0^2 = \frac{1}{k_B T} \frac{h^2}{2\pi\mu}, \tag{14}
$$

where μ is the reduced mass of the system. Moreover, in Eq. (13) the frequency argument of the spectral function is expressed in cm^{-1} by introducing the wavenumber notation, $\nu \equiv \omega/2\pi c$, in order to make it more consistent with the convention widely used in other works. Hence, the absolute spectral intensity values, $\mathcal{J}_{iso}(\nu)$, finally derived are denominated in cm^6 (in CGS).

2. Semi-classical calculations

The translational profiles can be also calculated efficiently by means of the methods based on solving the classical equations of motion along the trajectories of the colliding molecular subsystems. The core quantity obtained in this manner, the time correlation function of the particular SA components of the isotropic collisional polarizability[85]

$$
\begin{aligned}
{}^{(L)}S^{tr}(t) = \frac{4\pi}{2L+1} \sum_{\lambda} \big\langle \Delta\alpha^{(0)}_{\lambda\lambda}(R(0))\, \mathbf{Y}_L\big(\widehat{\boldsymbol{R}}(0)\big) \\
\odot \Delta\alpha^{(0)}_{\lambda\lambda}(R(t))\, \mathbf{Y}_L\big(\widehat{\boldsymbol{R}}(t)\big) \big\rangle,
\end{aligned}
\tag{15}
$$

can be subsequently applied to evaluate its Fourier transforms immediately associated with the spectral intensities needed. To put it more precisely, while the classical spectra due to the free molecular pair interactions are considered, the basic standard procedure is applied based on the preliminary calculation of the molecular trajectories versus velocity and impact parameter.[1,85] On doing that, the translational contribution to

the intensity (Eq. (8)) can be obtained in the following form:

$$ {}^{(cl)}g^{(0)}_{\lambda\lambda}(\nu) = c\int_0^\infty \left(\frac{\mu}{2\pi k_B T}\right)^{\frac{3}{2}} \exp\left(-\frac{\mu s^2}{2k_B T}\right) 4\pi s^3 ds \times \int_0^\infty \Delta\tilde{\alpha}^{(0)}_{\lambda\lambda}(b,s,\nu) 2\pi b\, db, \quad (16)$$

where the impact parameter is denoted by b, while s stands for the relative velocity of a collisional encounter. The functions $\Delta\tilde{\alpha}^{(0)}_{\lambda\lambda}(b,s,\nu)$ are obtained by calculating time integrals along the classical trajectories. For instance, a relevant expression for the most significant SA contribution to the central frequency interval of the isotropic spectra reads

$$ \Delta\tilde{\alpha}^{(0)}_{00}(b,s,\nu) = 4\left(\int_0^\infty \Delta\alpha^{(0)}_{00}(t,s,b)\cos(2\pi\nu t)dt\right)^2. \quad (17)$$

For a more detailed description of the numerical procedures and general formulas the reader is referred to Refs. 1, 48, and 85, and the references therein.

It may be worth noticing that it is also possible to consider the contribution of the pairs trapped in the well of the intermolecular potential (bound and meta stable dimers);[91] however for this work, it is not necessary because the latter, although it plays a role in the vicinity of the central Rayleigh line, is not significant in the Rayleigh wings. The classical spectra ${}^{(cl)}g^{(0)}_{\lambda\lambda}(\omega)$ are obtained in absolute units (cm^{10}, in the CGS unit system). So, it is possible to check that the integrals of the quantities ${}^{(cl)}g^{(0)}_{\lambda\lambda}(\omega)\,\omega^{2n}$ correspond to classical spectral moments $M^{(cl)}_{2n}$ obtained by using the sum rules.

Then, the spectra are desymmetrized by multiplying by appropriately designed functions. Namely, they are linear combinations of three desymmetrization functions available in the literature.[42] The coefficients of these combinations are obtained by fitting from the comparison of the successive moments of the desymmetrized spectra ${}^{(cl)}g^{(0)}_{\lambda\lambda}(\omega)$ with corresponding semi-classical spectral moments M^{sc}_n.[92] By doing that, one can evaluate semi-classical spectral lines precisely reproducing the quantum nature of the phenomena considered, which makes them a perfect yardstick for gauging the accuracy of profiles obtained by means of other methods.

B. Close-coupling calculations: The role of the anisotropic potential components

The computing approach applied in Secs. V A 1 and V A 2 is based on the H_2–Rg interaction model, in which the potential is treated as an almost isotropic property determined exclusively by the angle independent contribution to the expansion given in Eq. (6), V_0. Hereafter, an analysis is performed in order to find out to what extent this approximation may serve as a justifiable assumption with regard to the processes discussed in this work. To this end, a well-known, the so-called close-coupling, scheme of integrating the Schrödinger equation is applied,[49] by which the anisotropic aspect of the interactions can be taken into consideration. Within the CC procedures, the light scattering intensity can be represented by[11]

$$ \mathcal{J}_{iso}(\nu) = \frac{c\lambda_0^3\nu_s^2}{\phi_0\phi_s h}\sum_{\alpha_i}\frac{g_{j_i}\exp\left(-E^{rot}_{j_i}/k_B T\right)}{Z} \times \int_0^\infty dE_i e^{-E_i/k_B T}\left|S^{\alpha_f 01}_{\alpha_i 10}(E_i)\right|^2, \quad (18)$$

where the photon fluxes for the incident and scattered light are ϕ_0 and ϕ_s, respectively. Assuming that the radiative coupling is weak and using a partial wave expansion for the scattering wave functions yields the coupled radial Schrödinger equation[11,40]

$$ \left\{E^{\rm rot}_{j''} - \frac{\hbar^2}{2m}\frac{d^2}{dR^2} + \frac{\hbar^2 l''(l''+1)}{2mR^2} + n'_0\hbar\omega_0 + n'_s\hbar\omega_s - E\right\} \times F^{\alpha n_0 n_s}_{\alpha'' n'_0 n'_s}(R;E)\delta_{n'_0,1-n'_s} + \sum_{\alpha'} V_{\alpha''\alpha'}(R)F^{\alpha n_0 n_s}_{\alpha'' n'_0 n'_s}(R;E)\delta_{n'_0,1-n'_s} + \sum_{\alpha'} W_{\alpha''\alpha'}(R)F^{\alpha n_0 n_s}_{\alpha'' n'_s n'_0}(R;E)\delta_{n'_0,1-n'_s} = 0, \quad (19)$$

where n_0, n'_0 and n_s, n'_s designate the photon numbers of the incident and scattered fields, respectively, and the corresponding angular frequencies are ω_0 and $\omega_s = 2\pi c\nu_s$. The short hand notation $\alpha = (j, l, J)$ has been used for the angular momentum quantum numbers corresponding to $\boldsymbol{J} = \boldsymbol{j} + \boldsymbol{l}$, i.e., the total angular momentum being the sum of rotational and translational angular momenta. The total energy is $E = E_i + E^{\rm rot}_{j_i} + \hbar\omega_0 = E_f + E^{\rm rot}_{j_f} + \hbar\omega_s$, where E_i and E_f are the initial and final asymptotic kinetic energies, respectively. There are also certain approximating conditions assumed concerning the basic parameters of the routine. For instance, the initial H_2 rotations included correspond to j_i values of 0, 1, 2, and 3, whereas the final states are characterized by $j_f = 0, 2, 3, 4, 5$. The maximum total angular momentum J is equal 40. Moreover, closed channels are included on condition that the total energy is less than 400 cm^{-1} below the channel's asymptotic energy.

The asymptotic solutions of Eq. (19) give the scattering matrix elements $S^{\alpha_f 01}_{\alpha_i 10}$ corresponding to Raman scattering through the coupling W (see, e.g., Ref. 93).

When there are no vibrational transitions during the radiation process, the matrix elements of the interaction potential described by Eq. (6) are

$$ V_{\alpha\alpha'}(R) = \sum_\gamma \langle v=0|V_\gamma(R,r)|v=0\rangle\; f_\gamma(j,l,j',l';J)\,\delta_{JJ'} \quad (20)$$

with the coefficients[94]

$$ f_\gamma(j,l,j',l';J) = (-1)^{j+j'-J}[j][l][j'][l']\begin{Bmatrix} j & l & J \\ l' & j' & \gamma\end{Bmatrix} \times \begin{pmatrix} l & l' & \gamma \\ 0 & 0 & 0\end{pmatrix}\begin{pmatrix} j & j' & \gamma \\ 0 & 0 & 0\end{pmatrix}. \quad (21)$$

The polarized light scattering coupling due to the interaction induced trace is

$$W_{\alpha\alpha'}(R) = \sqrt{\frac{2\pi\hbar\omega_0\phi_0}{c}}\sqrt{\frac{2\pi\hbar\omega_s\phi_s}{c}} \times \sum_{\lambda L}(-)\sqrt{\frac{1}{3}}\Delta\alpha^{(0)}_{\lambda L}(R)d^{(0)}_{\lambda L}(j,l,J,j',l',J)\,\delta_{JJ'}, \tag{22}$$

where the coefficients d are defined by

$$d^{(K)}_{\lambda L}(j,l,J,j',l',J') = \frac{(-)^{l+j+J}}{[K]}[j][j'][l][l'][J][J'][\lambda][L] \times \begin{pmatrix} l & L & l' \\ 0 & 0 & 0 \end{pmatrix}\begin{pmatrix} j & \lambda & j' \\ 0 & 0 & 0 \end{pmatrix}\begin{Bmatrix} j' & l' & J' \\ j & l & J \\ \lambda & L & K \end{Bmatrix}, \tag{23}$$

where $[X] \equiv \sqrt{2X+1}$.

The procedure presented in this section can be easily adapted to the situation, when the potential is considered as isotropic. As a consequence, the numerical results could be compared accordingly with those yielded by the IPA methods discussed before. In such a case, the S-matrix elements can be conveniently computed with the distorted wave approximation.[49] With energy normalization[90] of the wave functions F the squared scattering matrix elements are

$$|S^{\alpha_f 01}_{\alpha_i 10}(E_i)|^2 = 4\pi^2\frac{2\pi\hbar\omega_0\phi_0}{c}\frac{2\pi\hbar\omega_s\phi_s}{c}\left\{[j_i][l_i][j_f][l_f]\right\}^2 \times \sum_{\lambda L}\begin{pmatrix} j_i & \lambda & j_f \\ 0 & 0 & 0 \end{pmatrix}^2\begin{pmatrix} l_i & L & l_f \\ 0 & 0 & 0 \end{pmatrix}^2 \times \left[\int dR F^*_{\alpha_i 10}(R;E_i)\Delta\alpha^{(0)}_{\lambda L}(R)F_{\alpha_f 01}(R;E_f)\right]^2. \tag{24}$$

The wave radial wave functions $F_{\alpha_i 10}$ and $F_{\alpha_f 01}$ are the solutions of Eq. (19), where only the potential components with $\gamma = 0$ are included and the radiative couplings $W_{\alpha\alpha'}$ have been excluded. In this case, the angular momentum quantum numbers are $\alpha = (j, l)$: The total angular momentum quantum number J_i and J_f are implicitly summed over in the derivation of Eq. (24) (see, e.g., Ref. 88). The final form of Eq. (24), when substituted in Eq. (18), results in the expression equivalent to the IPA intensity determined with Eqs. (10)–(13).

VI. RESULTS, FINAL REMARKS, AND ANALYSIS

The focus of the present study was on a collective electrical property—the trace polarizability—induced in systems composed of hydrogen molecules interacting with noble gas atoms, Rg = He, Ne, Ar, Kr, Xe. A quantum chemistry *ab initio* method was proposed and applied to determine the components of this quantity, which entered calculations of isotropic light scattering spectra. The programme was formulated with the goal that the means developed and the results obtained should pave the way for experimental works based on methods that have been developed in molecular spectroscopy throughout recent decades. Therefore, the presented research included thorough and precise theoretical and numerical calculations of data suitable for interpretation of experimental observables. To this end, assuming initially an isotropic potential between H_2 and Rg, the collisional spectra were found. Three independent methods for calculation of the line shapes were employed in order to provide appropriate benchmarking criteria for experimentally accepted accuracy. Among them, a semi-classical method was used to calculate relative trajectories of the moieties of the pairs, and subsequently their correlation and appropriate Fourier transform found. In the second approach, the relevant Schrödinger equation for the center of mass of H_2–Rg was solved quantum-mechanically. Then the matrix elements of the trace of polarizability were calculated. Eventually, very accurate CC calculations were used in the isotropic potential approximation and additionally, taking into account the anisotropy of the H_2–Rg pairs. This method led us to the absolute spectra for all H_2–Rg pairs.

The numerical results are presented partially in a tabularized form on the web site http://zon8.physd.amu.edu.pl/tbancewi (polarizability components) and in a more qualitative manner in Figs. 1–11. The outcome of the three methods of computing the ICIS profiles is illustrated in Figs. 6–10. In Figs. 6 and 8, the discrete points mark the IPA CC results plotted against the QM total lines. The two data sets are consistent to the level of convergence of the calculations, particularly in the frequency range of expected experimental interest (between 10 and 500 cm^{-1}), with the relative deviation ranges from negligible values to not much more than 3% . The semi-classical points are inserted in Fig. 7 (Rg = Ne) for the most pronounced spectral line assigned to the λ, L = 00 SA polarizability component. The difference compared with the QM result does not exceed 6% and the same applies to the heavier compounds (Rg = Kr and Xe, Figs. 9 and 10), with a few

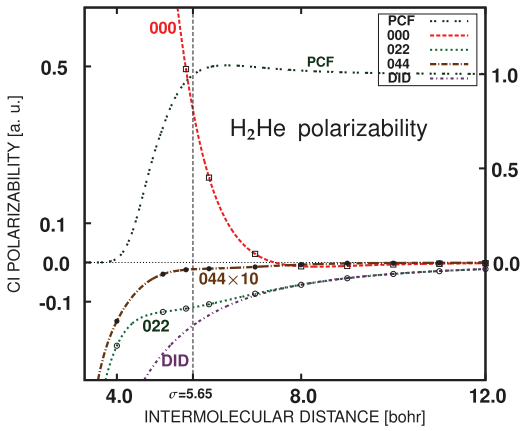

FIG. 1. Collisional symmetry adapted components of the isotropic polarizability, $\Delta\alpha^{(0)}_{\lambda L}(R)$ (expressed in atomic units); H_2–He case. Curves are identified by $0\lambda L$ values. Lines represent analytical functional dependence on intermolecular distance R obtained by fitting to *ab initio* data. Original QC results are indicated as discrete sets of points. The function represented analytical DID values is additionally depicted. The diameter of collision σ is marked and the pair correlation function illustrated. The 044 component is artificially enhanced so that it could be more distinguishable.

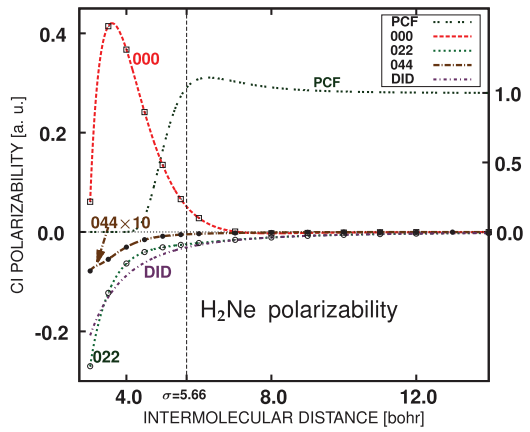

FIG. 2. The same as in Fig. 1, though for the H_2–Ne polarizability.

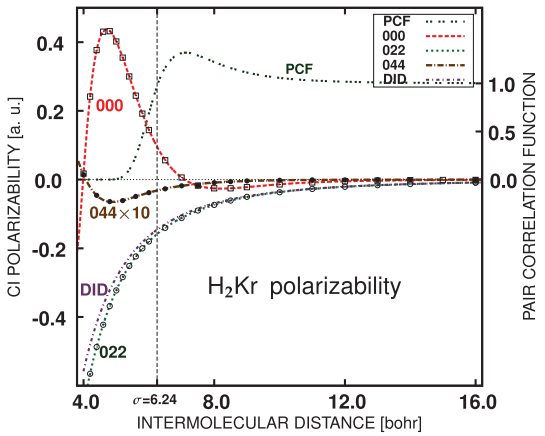

FIG. 4. The same as in Fig. 1, though for the of H_2–Kr polarizability.

exceptions at large frequency shifts. Assuming that there is always a leeway for further adjustment of the computing code, it must be admitted that the methods have proven a reliable tool to obtain relevant and accurate collisional spectra.

Besides, the CC method was used to consider a possible influence of the potential anisotropy on the spectral intensities. As the considered pairs contain a small percentage of high symmetry supermolecules, it is usually assumed that an approach like the CC routines should yield only a small deviation from the former results. Indeed, the lines compared in Fig. 11 deviate in barely noticeable way at a maximum rate of around 2%–3% in H_2–He to 6% in H_2–Ar. Possibly, the discrepancy increases with growing mass of the pairs, which may suggest more careful treatment of the anisotropy while dealing with heavier compounds.

Apart from the above, several other observations seem to be worth mentioning here concerning both the overall total profiles and their particular SA-related contributions as well as the mechanisms inducing the particular elements of the line shapes. As far as the intensities are considered, a careful examination of the CI isotropic spectra for the H_2–Rg sequence (Rg = He, Ne, Ar, Kr, Xe) reveals that a substantially higher spectrum is obtained as the polarizability of the Rg atom increases when moving from He to Xe. The change is significant: an order of magnitude from H_2–He to H_2–Xe. However, not all of the SA-related components (denoted from now on as: 000, 022, and 044) participate in the same way in building up the spectral magnitudes. For instance, the 044 contribution is virtually meaningless in this respect in the most frequency ranges except for the experimentally inaccessible side parts in the far wings. This notion, on the one hand, may justify reducing the relevant series expansions in Eq. (3) to the terms not exceeding the level of $\lambda = 4$. On the other hand, judging at the face value from the figures presented, even the 044 intensities may be safely skipped in further analysis. As for the two remaining components, 000 and 022, their influence should be mostly scrutinized within the spectral regions usually regarded as experimentally attainable frequency intervals–up to several hundreds of cm^{-1} around the central ($\nu = 0$ cm^{-1}) peak.[4–7,10,12] In this respect, a distinction can be drawn between two subsets of the scattering compounds. For the least massive/polarizable systems, with Rg = He and Ne atoms (Figs. 6 and 7), the purely translational contribution 000 almost exclusively forms the central part of the total profile, with only a small influence of the first 022 rotational transition line barely marked at about $\nu = 360$ cm^{-1}. It is only within the frequencies exceeding about 600 cm^{-1}, where the 022 ingredient takes precedence over its 000 counterpart and tends to dominate for the higher frequencies. However, the picture changes significantly, when more polarizable systems

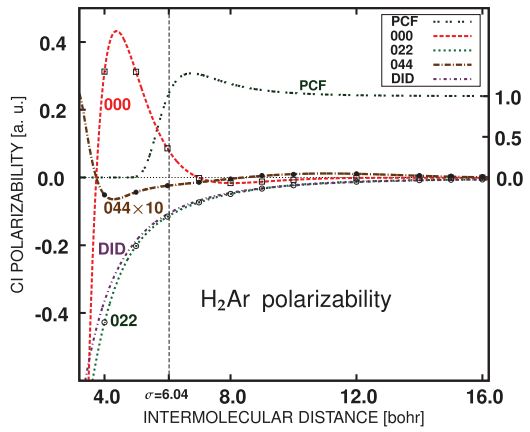

FIG. 3. The same as in Fig. 1, though for the H_2–Ar polarizability.

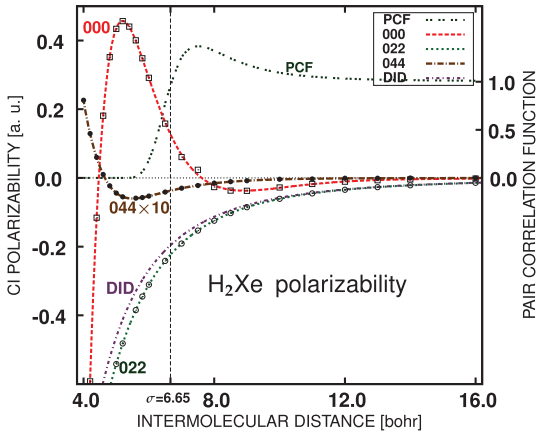

FIG. 5. The same as in Fig. 1, though for the of H_2–Xe polarizability.

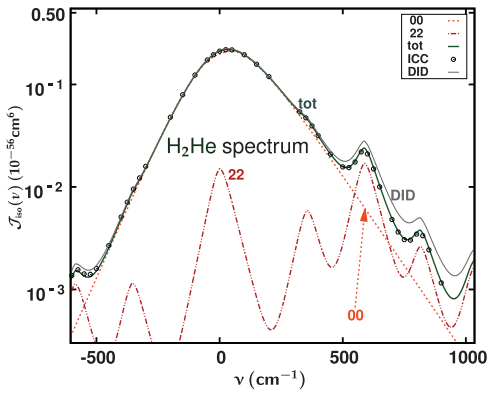

FIG. 6. Roto-translational ICIS spectral profile related to H_2–He polarizability (at temperature T = 295 K). Solid line depicts total intensity distribution (tot) obtained by quantum-mechanical computations; discrete points show close-coupling results, isotropic potential approximation (ICC). Additional shape marked with 00 represents the contribution related to $\lambda L = 00$ symmetry adapted component, while 22 and 44 are $\lambda = 2$ and 4 spectral SA shares, respectively.

(Rg = Ar, Kr, and Xe) are taken into account. For them, both the 000 and 022 parts give rise to the total spectra at almost equivalent rates for the frequencies below the 500 cm^{-1} limit. Again, above this point the latter part very quickly starts to overcast the 000 intensities.

A glimpse at Figs. 1–5, along with knowledge of several earlier analyzes (e.g., in Refs. 6, 7, 10, and 12), may provide insight into the behavior of the ICIS spectra. First, it must be noted that the collisional mechanisms responsible for the 000 share are of typically quantum nature, i.e., the overlap and/or exchange short-range interactions partially supplemented by the dispersion forces. On the other hand, the lowest order, dipole-induced-dipole (DID) multipolar mechanism affects the polarizability at more remote distances and, by symmetry requirements, is active only in the 022 case.[31,33] As it can be seen form Figs. 1 and 2, the *quantum-like* interactions produce an overwhelming portion of the trace polarizability, mostly enhancing its 000 share, within a relatively extended, yet rather short-distance, interval of intermolecular distances. Even more so, these effects additionally mark their influence by reducing the absolute values of the 022 component. Another evidence of this "destructive" role is provided in Fig. 6, where a profile evaluated by including only the bare

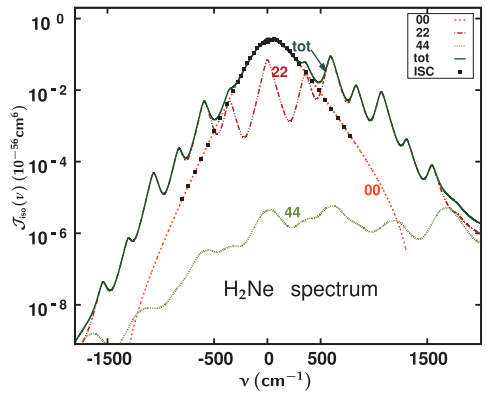

FIG. 7. The same as in Fig. 6 for the spectrum of the H_2–Ne mixture, except that the points represent the semi-classical 00 intensities (ISC).

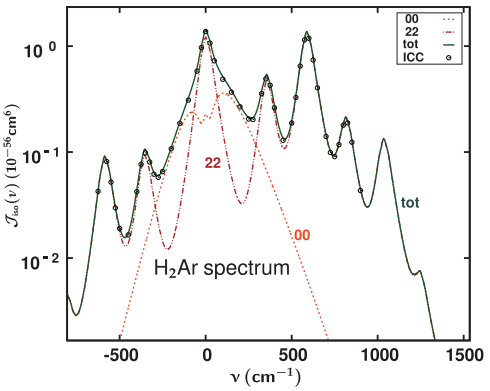

FIG. 8. The same as in Fig. 6, yet for the spectrum of the H_2–Ar mixture.

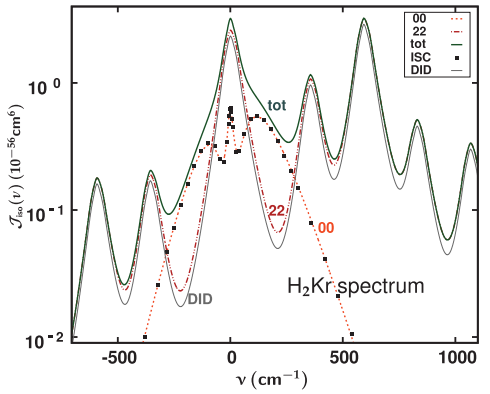

FIG. 9. The same as in Fig. 7, yet for the spectrum of the H_2–Kr mixture.

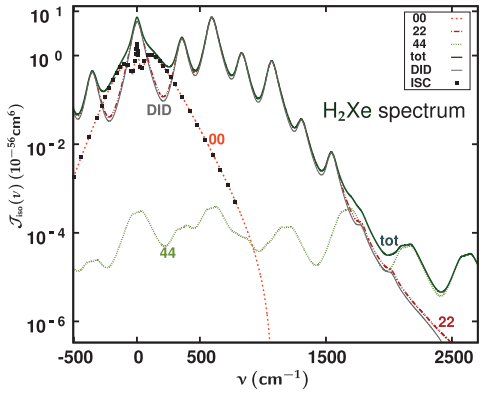

FIG. 10. The same as in Fig. 7, yet for the spectrum of the H_2–Xe mixture.

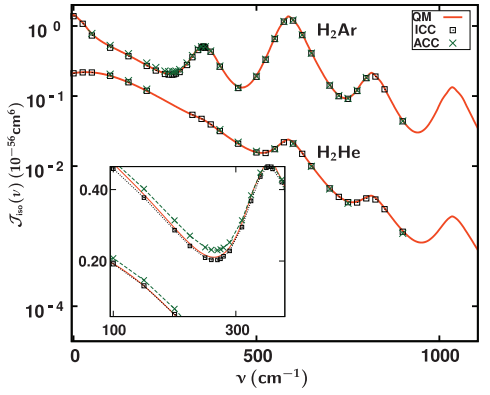

FIG. 11. Comparison between the ICIS spectral profiles: isotropic potential case (solid lines and squares, respectively) and the CC results with the anisotropic potential applied (crosses).

DID contribution to the 022 lines exhibits a shape substantially divergent from that obtained on the basis of the full *ab initio* approach (tot).

The above conclusions concerning the lightest, the most "quantum-like" supermolecules, especially H_2–He mixtures, support the observations made in earlier CIS study of light scattering separately in the hydrogen and helium species.[6] The H_2–Rg compounds seem to share the spectral features of the constituent moieties. On the one hand, the profiles show a strong dependence on the short distance quantum interactions in the most central and relatively broad part, although the influence of more distant correlations should not be neglected as they tend to dominate in the adjacent frequency region. Nevertheless, for the spectral sections that might be of the most experimental importance, the domineering role of the 000 component is evident and the influence of the 022 intensities is to some extent negligible; an interesting feature that could be possibly used in attempts of extracting data characterizing a "pure" quantum mechanisms inducing the collisional trace polarizability.

Another interpretation is supposedly applicable for the more polarizable H_2–Rg compounds as the spectral properties reveal a kind of evolutionary modification with growing supermolecular masses towards a state of more balanced share in the total intensities attributed to each of the 000 and 022 components. Analogously, this tendency corresponds to the features of the symmetry adapted polarizability components illustrated in Figs. 3–5. Now, the magnitudes of the 022 intensities became more pronounced in comparison with the 000 values, beginning from relatively short intermolecular distances. Moreover, the long range DID model fits more closely to the *ab initio* originated lines, although even for the heaviest, H_2–Xe, system the multipolar approach is not able to reproduce precisely enough the *ab initio* shapes. In Fig. 10, the DID related profile plotted in the log scale qualitatively follows much better the *ab initio* shape pattern than its counterpart in H_2–He (Fig. 6), yet in fact, the calculated discrepancies may reach the level of between 10% and 25% within the frequencies crucial for formation of the rotational spectral structures.

The above remarks should shed light onto several questions raised on the basis of the present results. Nevertheless, only when supplemented with solid reliable experimental data, they could give real insight into ICIS. Therefore, major challenges ensue this investigation. These are primarily the measurement of CI induced spectra for H_2–Rg by experimentalists, the calculation of similar spectra for other systems by theoretical spectroscopists and last the calculation of accurate interaction-induced electric properties by computational quantum chemists methods. Work is now in progress on other similar systems.

[1] L. Frommhold, Adv. Chem. Phys. **46**, 1 (1981).
[2] J. P. McTague and G. Birnbaum, Phys. Rev. Lett. **21**, 661 (1968).
[3] M. H. Proffitt and L. Frommhold, J. Chem. Phys. **74**, 1512 (1981).
[4] U. Bafile, L. Ulivi, M. Zoppi, F. Barocchi, M. Moraldi, and A. Borysow, Phys. Rev. A **42**, 6916 (1990).
[5] U. Bafile, L. Ulivi, M. Zoppi, and F. Barocchi, Phys. Rev. A **37**, 4133 (1988).
[6] L. Frommhold, J. D. Poll, and R. H. Tipping, Phys. Rev. A **46**, 2955 (1992).
[7] M. H. Proffitt, J. W. Keto, and L. Frommhold, Can. J. Phys. **59**, 1459 (1981).
[8] O. Gaye, M. Chrysos, V. Teboul, and Y. LeDuff, Phys. Rev. A **55**, 3484 (1997).
[9] S. Dixneuf, M. Chrysos, and F. Rachet, Phys. Rev. A **80**, 022703 (2009).
[10] M. S. Brown, S. K. Wang, and L. Frommhold, Phys. Rev. A **40**, 2276 (1989).
[11] M. Gustafsson, L. Frommhold, X. Li, and K. L. C. Hunt, J. Chem. Phys. **130**, 164314 (2009).
[12] M. S. Brown and L. Frommhold, Mol. Phys. **66**, 527 (1989).
[13] P. Benassi, V. Mazzacurati, M. Nardone, M. A. Ricci, G. Ruocco, A. DeSantis, R. Frattini, and M. Sampoli, Mol. Phys. **62**, 1467 (1987).
[14] A. DeSantis, R. Frattini, M. Sampoli, and R. Vallauri, Europhys. Lett. **2**, 17 (1986).
[15] A. DeSantis and M. Sampoli, Chem. Phys. Lett. **102**, 425 (1983).
[16] A. DeLorenzi, A. DeSantis, R. Frattini, and M. Sampoli, Phys. Rev. A **33**, 3900 (1986).
[17] T. Bancewicz, V. Teboul, and Y. LeDuff, Mol. Phys. **81**, 1353 (1994).
[18] T. Bancewicz, K. Nowicka, J.-L. Godet, and Y. LeDuff, Phys. Rev. A **69**, 062704 (2004).
[19] T. Bancewicz, J.-L. Godet, and G. Maroulis, J. Chem. Phys. **115**, 8547 (2001).
[20] K. Nowicka, T. Bancewicz, J.-L. Godet, F. Rachet, and Y. LeDuff, Mol. Phys. **101**, 389 (2003).
[21] T. Bancewicz, Y. LeDuff, and J.-L. Godet, *Modern Nonlinear Optics., Part 1*, 2nd ed., edited by M. Evans (J. Wiley, New York, 2000), p. 89.
[22] D. Kremer, F. Rachet, and M. Chrysos, J. Chem. Phys. **138**, 174308 (2013).
[23] G. Maroulis, J. Phys. Chem. A **104**, 4772 (2000).
[24] G. Maroulis and A. Haskopoulos, Chem. Phys. Lett. **349**, 335 (2001).
[25] G. Maroulis and A. Haskopoulos, Chem. Phys. Lett. **358**, 64 (2002).
[26] A. Haskopoulos, D. Xenides, and G. Maroulis, Chem. Phys. Lett. **309**, 271 (2005).
[27] S. Dixneuf, M. Chrysos, and F. Rachet, J. Chem. Phys. **131**, 074304 (2009).
[28] X. Li, C. Ahuja, J. F. Harrison, and K. L. C. Hunt, J. Chem. Phys. **126**, 214302 (2007).
[29] X. Li, J. F. Harrison, M. Gustafsson, L. Frommhold, and K. L. C. Hunt, *A Homage to the Pioneering Work of Stanisław Kielich (1925-1993)*, edited by G. Maroulis, T. Bancewicz, B. Champagne, and A. D. Buckingham (IOS Press, Amsterdam, 2011).
[30] M. J. Frisch, G. W. Trucks, H. B. Schlegel *et al.*, gaussian 03, Revision D.01, Gaussian, Inc., Wallingford, CT, 2004.
[31] T. Bancewicz and G. Maroulis, Chem. Phys. Lett. **471**, 148 (2009).
[32] T. Bancewicz and G. Maroulis, Phys. Rev. A **79**, 042704 (2009).
[33] T. Bancewicz, J. Chem. Phys. **134**, 104309 (2011).
[34] J. E. Dove, A. C. M. Rusk, P. H. Cribb, and P. G. Martin, Astrophys. J. **318**, 379 (1987).
[35] L. M. Trafton, in *Molecular Complexes in Earth's, Planetary, Cometary and Interstellar Atmospheres*, edited by A. A. Vigasin and Z. Slanina (World Scientific, Singapore, 1998).
[36] A. Borysow and M. Moraldi, Phys. Rev. A **40**, 1251 (1989).
[37] A. Borysow and M. Moraldi, Phys. Rev. A **48**, 3036 (1993).
[38] X. Li, A. Mandal, E. Miliordos, and K. L. C. Hunt, J. Chem. Phys. **136**, 044320 (2012).
[39] M. Gustafsson and L. Frommhold, Phys. Rev. A **74**, 054703 (2006).
[40] M. Gustafsson, L. Frommhold, and W. Meyer, J. Chem. Phys. **113**, 3641 (2000).
[41] W. Głaz, T. Bancewicz, J. L. Godet, G. Maroulis, and A. Haskopoulos, J. Chem. Phys. **138**, 124307 (2013).
[42] T. Bancewicz, W. Głaz, J.-L. Godet, and G. Maroulis, J. Chem. Phys. **129**, 124306 (2008).
[43] W. Glaz, J. L. Godet, A. Haskopoulos, T. Bancewicz, and G. Maroulis, Phys. Rev. A **84**, 012503 (2011).
[44] J. L. Godet, T. Bancewicz, W. Glaz, G. Maroulis, and A. Haskopoulos, J. Chem. Phys. **131**, 204305 (2009).
[45] W. Głaz, Proc. SPIE **8697**, 869723 (2012).
[46] W. Głaz, J. Comput. Meth. Sci. Eng. **11**, 339 (2011).
[47] W. Głaz, T. Bancewicz, G. Maroulis, A. Haskopoulos, and J. L. Godet, J. Phys. Conf. Ser. **397**, 012044 (2012).
[48] W. Głaz, T. Bancewicz, J. L. Godet, G. Maroulis, and A. Haskopoulos, Phys. Rev. A **73**, 042708 (2006).
[49] P. S. Julienne, Phys. Rev. A **26**, 3299 (1982).
[50] B. J. Berne and R. Pecora, *Dynamic Light Scattering* (John Wiley and Sons, New York, 1976).
[51] V. Teboul, J. L. Godet, and Y. LeDuff, Appl. Spectrosc. **46**, 476 (1992).

[52]T. Bancewicz, Y. LeDuff, and J. L. Godet, "Multipolar polarizabilities from interaction-induced Raman scattering," in *Modern Nonlinear Optics, Part 1*, 2nd ed., edited by M. Evans (J. Wiley, New York, 2001), pp. 267–307.
[53]G. Maroulis, A. Haskopoulos, and D. Xenides, Chem. Phys. Lett. **396**, 59 (2004).
[54]A. Haskopoulos and G. Maroulis, J. Math. Chem. **40**, 233 (2006).
[55]A. D. Buckingham, Adv. Chem. Phys. **12**, 107 (1967).
[56]S. F. Boys and F. Bernardi, Mol. Phys. **19**, 553 (1970).
[57]J. O. T. Hergaker and P. Jorgensen, *Molecular Electronic-Structure Theory* (Wiley, Chichester, 2000).
[58]L. Frommhold, *Collision-Induced Absorption in Gases* (Cambridge University Press, Cambridge, 1993).
[59]C. G. Gray and K. E. Gubbins, *Theory of Molecular Fluids. Vol. 1: Fundamentals* (Clarendon Press, Oxford, 1984).
[60]C. G. Gray and B. W. N. Lo, Chem. Phys. **14**, 73 (1976).
[61]D. A. Varshalovich, A. N. Moskaliev, and V. K. Khersonskii, *Quantum Theory of Angular Momentum* (World Scientific, Singapore, 1988).
[62]P. Karamanis and G. Maroulis, Comput. Lett. **1**, 117 (2005).
[63]A. Baranowska, A. Zawada, B. Fernandez, W. Bartkowiak, D. Kedziera, and A. Kaczmarek-Kedziera, Phys. Chem. Chem. Phys. **12**, 852 (2010).
[64]A. Baranowska, B. Fernandez, and A. J. Sadlej, Theor. Chim. Acta **128**, 555 (2011).
[65]A. Zawada, A. Kaczmarek-Kedziera, and W. Baranowska, Chem. Phys. Lett. **503**, 39 (2011).
[66]A. Baranowska-Laczkowska, B. Fernandez, and R. Zalesny, J. Compt. Chem. **34**, 275 (2013).
[67]G. Maroulis, J. Chem. Phys. **113**, 1813 (2000).
[68]G. Maroulis, C. Makris, U. Hohm, and D. Goebel, J. Phys. Chem. A **101**, 953 (1997).
[69]G. Maroulis, Chem. Phys. **291**, 81 (2003).
[70]G. Maroulis, J. Chem. Phys. **105**, 8467 (1996).
[71]G. Maroulis, Chem. Phys. Lett. **259**, 654 (1996).
[72]M. J. Frisch, G. W. Trucks, H. B. Schlegel *et al.*, gaussian 98, Revision A.7, Gaussian, Inc., Pittsburgh, PA, 1998.
[73]A. Haskopoulos and G. Maroulis, Chem. Phys. **367**, 127 (2010).
[74]See Section II of Ref. 32, which leans heavily on the computational philosophy expanded in Ref. 23.
[75]J. Schaefer and W. E. Kohler, Physica A **129**, 469 (1985).
[76]M. Moraldi, A. Borysow, J. Borysow, and L. Frommhold, Phys. Rev. A **34**, 632 (1986).
[77]M. Gustafsson and L. Frommhold, Phys. Rev. A **63**, 052514 (2001).
[78]F. Lique, Chem. Phys. Lett. **471**, 54 (2009).
[79]H. L. Williams, K. Szalewicz, B. Jeziorski, R. Moszynski, and S. Rybak, J. Chem. Phys. **98**, 1279 (1993).
[80]R. J. LeRoy and J. M. Hutson, J. Chem. Phys. **86**, 837 (1987), and references therein.
[81]H. Posch, Mol. Phys. **37**, 1059 (1979).
[82]H. Posch, Mol. Phys. **40**, 1137 (1980).
[83]B. Guillot and G. Birnbaum, *Reactive and Flexible Molecules in Liquids*, edited by Th. Dorfmuüller (Kluver Academic Publishers, Dordrecht, 1989), pp. 1–36.
[84] R. Pleich, Ph.D. thesis, University of Viena, Vienna, 1983.
[85]H. Posch, Mol. Phys. **46**, 1213 (1982).
[86]A. R. Edmonds, *Angular Momentum in Quantum Mechanics* (Princeton University Press, 1957).
[87]G. Birnbaum, B. Guillot, and S. Bratos, Adv. Chem. Phys. **51**, 49 (1982).
[88]G. Birnbaum, S. Chu, A. Dalgarno, L. Frommhold, and E. L. Wright, Phys. Rev. A **29**, 595 (1984).
[89]W. Głaz and T. Bancewicz, J. Chem. Phys. **118**, 6264 (2003).
[90]L. D. Landau and E. M. Lifshitz, *Quantum Mechanics. Non-Relativistic Theory* (Pergamon Press, Oxford, 1965).
[91]N. Meinander, J. Chem. Phys. **99**, 8654 (1993).
[92]T. Bancewicz, W. Głaz, and J.-L. Godet, J. Chem. Phys. **127**, 134308 (2007).
[93]A. M. Arthurs and A. Dalgarno, Proc. Roy. Soc. A **256**, 540 (1960).
[94]W. A. Lester, Meth. Comput. Phys. **10**, 211 (1971).

Intermolecular polarizabilities in H2-rare-gas mixtures (H2–He, Ne, Ar, Kr, Xe): Insight from collisional isotropic spectral properties

Waldemar Gaz, Tadeusz Bancewicz, Jean-Luc Godet, Magnus Gustafsson, George Maroulis, and Anastasios Haskopoulos

Citation: The Journal of Chemical Physics **141**, 074315 (2014); doi: 10.1063/1.4892864
View online: http://dx.doi.org/10.1063/1.4892864
View Table of Contents: http://scitation.aip.org/content/aip/journal/jcp/141/7?ver=pdfcov
Published by the AIP Publishing